

Structural investigations of CeIrIn₅ and CeCoIn₅ on macroscopic and atomic length scales

Steffen Wirth,¹ Yurii Prots,¹ Michael Wedel,¹ Stefan Ernst,¹ Stefan Kirchner,^{2,1}

Zachary Fisk,³ Joe D. Thompson,⁴ Frank Steglich,¹ and Yuri Grin¹

¹Max Planck Institute for Chemical Physics of Solids, 01187 Dresden, Germany

²Max Planck Institute for Physics of Complex Systems, 01187 Dresden, Germany

³University of California, Irvine, California 92697, USA

⁴Los Alamos National Laboratory, Los Alamos, New Mexico 87545, USA

(Dated: February 22, 2022)

For any thorough investigation of complex physical properties, as encountered in strongly correlated electron systems, not only single crystals of highest quality but also a detailed knowledge of the structural properties of the material are pivotal prerequisites. Here, we combine physical and chemical investigations on the prototypical heavy fermion superconductors CeIrIn₅ and CeCoIn₅ on atomic and macroscopic length scale to gain insight into their precise structural properties. Our approach spans from enhanced resolution X-ray diffraction experiments to atomic resolution by means of Scanning Tunneling Microscopy (STM) and reveal a certain type of local features (coexistence of minority and majority structural patterns) in the tetragonal HoCoGa₅-type structure of both compounds.

Keywords: heavy-fermion metals, structural organization, electron density

I. INTRODUCTION

Heavy-fermion metals typically contain magnetic $4f$ or $5f$ elements (*e.g.* Ce, Yb or U) which give rise to magnetism of local moment character. At low temperatures, these magnetic moments can effectively be screened by conduction electrons due to the so-called Kondo effect [1]. The coupling of the free electrons to the localized f electrons can dramatically increase the effective mass of the charge carriers which may reach up to several hundred times the mass of a free electron. The properties of these metals can often be described, according to Landau [2], by considering quasi-particles made up of the electrons and their interactions—instead of the mere electrons—within the theory of a free electron gas. On the other hand, in many of these materials an indirect exchange coupling between the local magnetic moments is found (the so-called RKKY interaction) which is also mediated—just like the aforementioned Kondo interaction—via the conduction electrons. These two interactions are in direct competition. The relative strength of these two competing interactions can be tuned by experimental parameters such as chemical substitution, pressure and magnetic field. In case of this competition being adequately balanced a quantum phase transition (QPT) at $T = 0$ can be brought about by a well-directed change of these experimental parameters [3, 4].

Once the Kondo and RKKY interactions are well balanced additional, smaller energy scales may play a decisive role. In fact, in many cases superconductivity is observed in close proximity to a quantum critical point (QCP), *i.e.* the point in phase space at which a continuous QPT occurs [5]. Possibly, superconductivity is one way of disposing the huge entropy accumulated in the vicinity of a QCP. This concept has been generalized [6] such that possibly even in the copper-oxide materials superconductivity might be related to a hidden QCP. Here it should be noted that superconductivity for which such a scenario is discussed is commonly considered to be of unconventional nature, in a sense that the standard BCS theory employing phonon-mediated Cooper pair formation [7] can-

not be applied.

In this context the CeMIn₅ family of heavy-fermion compounds offers an interesting playground [8, 9]. The intricate interplay of superconductivity and magnetism is, *e.g.*, manifested by the existence of superconductivity found in CeCoIn₅ below the superconducting transition temperature $T_c \approx 2.3$ K, and antiferromagnetic order in CeRhIn₅ below the Néel temperature $T_N \approx 3.7$ K. Conversely, superconductivity with similar T_c is observed in the latter compound by the application of pressure [10] whereas neutron scattering experiments indicate strong antiferromagnetic quasielastic excitations in the paramagnetic regime of CeCoIn₅ [11]. Moreover, the existence of a field-induced QCP has been anticipated [12–17]. Also, in Cd-substituted CeCoIn₅ (*i.e.* CeCo(In_{1-x}Cd_x)₅ with $x \leq 0.01$) a microscopic coexistence and mutual influence of the superconducting and antiferromagnetic order via identical $4f$ states was inferred [18, 19].

We report on structural investigations by both, enhanced-resolution X-ray diffraction experiments as well as atomically resolved Scanning Tunneling Microscopy (STM) on single crystals of CeIrIn₅ and CeCoIn₅. These measurements indicate the existence of a certain type of local structural features in the tetragonal HoCoGa₅-type matrix that can directly be visualized by STM. These features can be considered as patches of the closely related TlAsPd₅ structure. They may also be related to the apparent discrepancy in bulk $T_c \approx 0.4$ K and resistive $T_c \approx 1.2$ K in CeIrIn₅ [20–22]. Our results obtained by Scanning Tunneling Spectroscopy (STS) confirm CeCoIn₅ to be a d -wave superconductor [23, 24] and indicate a precursor state to superconductivity above T_c as earlier inferred for CeIrIn₅ [22].

II. X-RAY DIFFRACTION

Normal-resolution neutron diffraction reported earlier [25] (540 symmetry dependent reflections, $R(F) = 0.051$) indicated that CeIrIn₅ crystallizes in the structure type HoCoGa₅ [26],

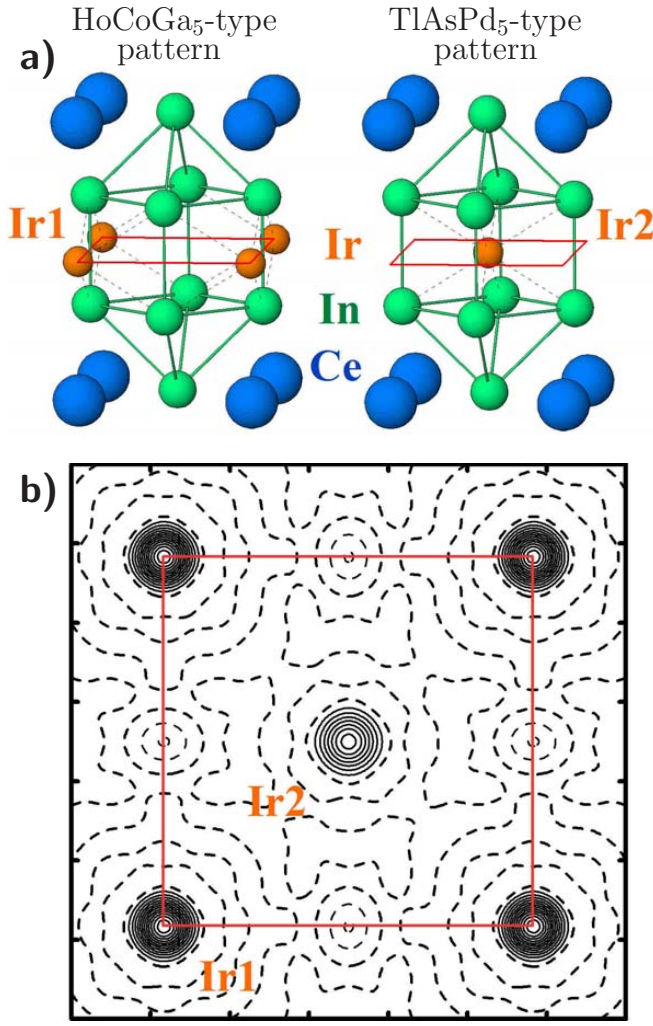


FIG. 1. a) Two closely related structure types HoCoGa₅ (left) and TlAsPd₅ (right). In the former structure, Ir occupies the position at $00\frac{1}{2}$ are occupied (Ir1). In comparison, the Ir2 position in the latter structure is shifted by $(\frac{1}{2}\frac{1}{2}0)$ within the $z = \frac{1}{2}$ plane. b) Difference electron density calculated from enhanced-resolution X-ray diffraction experiments on our single crystals of CeIrIn₅. This indicates the presence of about 1% of Ir in Ir2 positions (TlAsPd₅ pattern) at $z = \frac{1}{2}$ and hence, a coexistence of the two structural patterns in the crystal structure of CeIrIn₅ is inferred.

cf. Fig. 1(a) left. However, the results of the STM topography studies discussed below insinuated a more complex structure, at least at the sample surface. In an effort to possibly relate surface and bulk structural properties, we performed enhanced-resolution diffraction experiments on several samples CeIrIn₅ including those used for the STM investigations discussed below. Our X-ray diffraction experiments were conducted with a resolution comparable to the above-mentioned neutron investigations (Mo K α radiation, $2\theta_{\max} = 53^\circ$, 133 symmetry-independent reflections, $R(F) = 0.020$). In a first approximation, these experiments confirmed the crystal structure of the HoCoGa₅ type. Yet, recent investigations of the coexistence of different structural patterns in the modifications

of TmAlB₄ [27, 28] revealed the importance of the analysis of the difference electron density maps even in the case of a low residual value $R(F)$. Analysis of 232 symmetry-independent, non-zero intensity ($I \geq 2\sigma(I)$) reflections up to $2\theta_{\max} = 70^\circ$ (using Mo K α radiation) for CeIrIn₅ yielded $a = 4.6660(3)$ Å, $c = 7.5161(7)$ Å and the subsequent refinement resulted in $R(F) = 0.024$ within the space group $P4/mmm$. A striking feature of this refinement was the fact that the displacement parameter of Ir atoms (atomic number 77) is larger than the one for the more ‘light’ Ce (atomic number 58), which suggests a lower occupation of the Ir position. Indeed, the distribution of the difference electron density in the plane at $z = 0.5$, calculated from these diffraction data and without Ir atoms, exhibits maxima at the edges of the unit cell, see Fig. 1(b), positions marked Ir1. These maxima are expected for the structural pattern of the HoCoGa₅ type, Fig. 1(a) left. In addition, however, maxima of the difference electron density were also found in the center of the unit cell, *i.e.* at position Ir2, which is characteristic for the structure pattern of TlAsPd₅ type [29] (Fig. 1(a) right). Further refinement resulted in occupancies of $occ(\text{Ir1}) = 0.988(3)$ and $occ(\text{Ir2}) = 0.012(3)$.

As symmetry-averaged data were used, the refinement based on the unit weights required a fixed scale factor. The importance of the scaling on the stability of the refinement was already pointed out in the first structural study of CeIrIn₅ (Ref. 25). Because the crystal structure of the investigated crystals of CeIrIn₅ reveals a non-negligible disorder of the Ir atoms, the translational symmetry in strict sense is broken. Thus, we performed a more elaborate refinement of the crystal structure using all 1564 measured non-zero symmetry-dependent reflections (*i.e.* without averaging for symmetry equivalents). The standard deviations for the refined parameters were calculated using the number of the symmetry-independent reflections. In this case, the refinement was stable without fixing the scale factor (keeping goodness-of-fit, GOF, close to unity by an appropriate scaling) and yielded the occupancies of $occ(\text{Ir1}) = 0.989(3)$ and $occ(\text{Ir2}) = 0.011(3)$. Having in mind the importance of the completeness of the diffraction data set (*i.e.* the presence of *all* symmetrically equivalent reflections within the given range of $\sin \theta/\lambda$), we performed the final diffraction experiment on the same single crystal and obtained the completeness close to 100%, applying a specifically developed algorithm for collecting the diffraction data [30]. For the finally collected 1705 non-zero symmetry-dependent and the 240 non-zero symmetry-independent reflections (Mo K α radiation, $2\theta_{\max} = 70^\circ$) the refinement yielded the occupancies of $occ(\text{Ir1}) = 0.988(2)$ and $occ(\text{Ir2}) = 0.012(2)$ with $R(F) = 0.023$ and $occ(\text{Ir1}) = 0.984(2)$ and $occ(\text{Ir2}) = 0.016(2)$ with $R(F) = 0.016$, respectively. As the occupation values obtained in both cases agree within two estimated standard deviations, these values were averaged for the final model (Ref. 31). The presence of Ir atoms at two different positions is a key observation for understanding the atomic distribution on the surface as seen in the STM experiments.

Considering the similarities between CeIrIn₅ and CeCoIn₅ the existence of structure pattern of TlAsPd₅ type may also be expected in CeCoIn₅. The crystal structure of CeCoIn₅ was originally studied using X-ray powder diffraction data

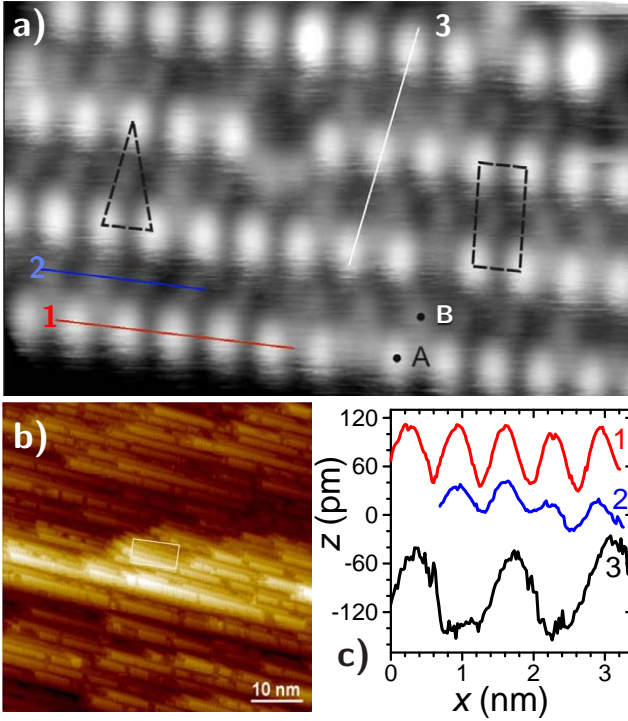


FIG. 2. a) STM topography on CeIrIn_5 after subtracting a plane with an inclination of 37° . The image covers an area of $5.4 \times 8.6 \text{ nm}^2$ and a total z -range of 0.63 nm . This image was obtained at $V_g = +600 \text{ mV}$, $I_{\text{set}} = 0.3 \text{ nA}$, $T = 330 \text{ mK}$. The markers **A** and **B** indicate two kinds of atomic corrugations. The dashed triangle and rectangle illustrate the two different arrangements of atoms of type **A**. Lines 1 and 3 involve atoms of type **A**; line 2 those of type **B**. b) Topography overview after subtracting a plane of 37° . The area shown in a) is marked. c) Line scans indicated in a).

[32] with no irregularities in the crystal structure reported. However, our enhanced-resolution single crystal diffraction experiment on CeCoIn_5 ($\text{Mo K}\alpha$ radiation, $2\theta_{\text{max}} = 66.4^\circ$, 1001 observed symmetry-dependent reflections) revealed occupancies of both possible Co positions (Co1 at $00\frac{1}{2}$ and Co2 at $\frac{1}{2}\frac{1}{2}\frac{1}{2}$) with the occupancy factors of $\text{occ}(\text{Co1}) = 0.985(8)$ and $\text{occ}(\text{Co2}) = 0.015(8)$ (Ref. 33). Despite the higher standard deviations caused by a lower contribution of cobalt atoms to the overall diffraction intensity, also here the refinement was stable including all observed reflections when keeping the goodness-of-fit close to unity by appropriate scaling.

III. STM INVESTIGATIONS OF SURFACE TOPOGRAPHY

In an attempt to directly visualize the crystal structure as well as the disorder discussed above we conducted topography measurements by STM. Because STM is a particularly surface sensitive technique special attention has to be paid with respect to the sample surface quality. Therefore, the STM utilized here is operated in UHV ($p \leq 2 \times 10^{-9} \text{ Pa}$) and equipped for *in situ* sample cleaving. Moreover, this STM can be operated at sample temperatures as low as 0.3 K (allowing for

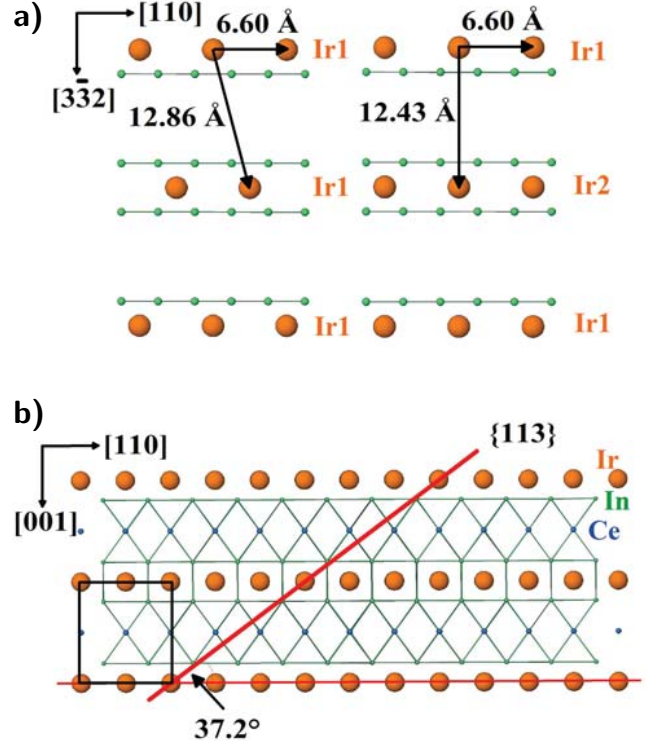


FIG. 3. a) Arrangement of the Ir and In atoms in the $\{113\}$ planes of the HoCoGa_5 (left) and the TlAsPd_5 structure (right). b) Visualization of a $\{113\}$ plane and its inclination angle with respect to the (001) plane.

an energy resolution of $\leq 100 \mu\text{eV}$) and in magnetic fields of up to 12 T . We stress again that in order to allow for a direct comparison between the results obtained by XRD and STM identical samples have been investigated.

Atomically resolved images of CeIrIn_5 were obtained within areas of up to $60 \times 60 \text{ nm}^2$, exhibiting various terraces of up to a few ten nm in extent [34], as exemplified in Fig. 2. In case of the overview topography presented in Fig. 2(b), a plane of inclination of 37° was subtracted. An area within a terrace marked in Fig. 2(b) is magnified in Fig. 2(a) and clearly shows atomic resolution. The sample was mounted parallel to the crystallographic ab -plane. Hence, the large value of the tilting angle of 37° of the imaged sample area with respect to the scanning plane points towards the fact that the terrace of Fig. 2(a) represents a lattice plane of low symmetry (we emphasize that this plane correction was taken into consideration when calculating the interatomic distances below). Note that this tilting of the area presented in Fig. 2(a) is maximum in a direction perpendicular to scan lines 1 and 2. Line scans through the prominent corrugations are presented in Fig. 2(c) and marked 1 and 3; the locations of these scans are indicated in Fig. 2(a). The distance between the corrugations depends strongly on the direction, $\sim 6.7 \text{ \AA}$ for line 1 and $\sim 13.7 \text{ \AA}$ for line 3. Given these distances it is unlikely that these prominent corrugations represent In atoms (at least as long as there is no severe surface reconstruction). The positive bias voltage $V_g = +600 \text{ mV}$ used while acquiring the topog-

raphy of Fig. 2(a) may support a more prominent visualization of Ir atoms since they accumulate the strongest negative charge. Therefore, the most prominent corrugations marked by **A** in Fig. 2(a) are probably Ir atoms. The corrugations marked as **B** could then originate from the Ce atoms of the intermittent Ce layers as shown in Figs. 3(a) and (b). This is corroborated by similar distances between the corrugations of type **B** (line 2) and of type **A** (line 1). Clearly, for corrugations of type **B** the assignment to a certain atomic species is even more problematic than for those of type **A** because, in addition to the actual height, also a changed density of states (DOS) may affect the apparent height. However, in what follows a reversed assignment of corrugations **A** to Ce and corrugations **B** to Ir would not significantly change our conclusions.

A tilting angle away from the $\{001\}$ plane is of importance for the possible identification of positions Ir1 and Ir2. Cleaves on the related compound CeCoIn_5 resulted in $\{001\}$ terminating planes [23, 24, 35]. However, within the $\{001\}$ plane the two positions Ir1 and Ir2 are difficult to distinguish because of the aforementioned shift of Ir planes.

IV. STRUCTURAL CONSIDERATIONS

The effective atomic charges in CeIrIn_5 were calculated applying the QTAIM (Quantum Theory of Atoms in Molecules [36]) approach. As expected from the electronegativities of the elements, Ir carries the largest negative charge (-1.7), In atoms have charges close to zero ($+0.25$ for In1 and -0.1 for In2), and Ce sustains the largest positive charge of $+0.8$. Taking this into account, the formula of the compound should—from a chemical point of view—be rather written as CeIn_5Ir ; yet for historical reasons we continue to use the ‘traditional’ formula CeIrIn_5 (as well as CeCoIn_5) in this work.

Further analysis of the chemical bonding in CeIrIn_5 (HoCoGa₅ type) applying the electron localizability approach [37] reveals that the Ir and In atoms form three-dimensional framework polyanions through the covalent (polar) three-center (3c) interactions. Three independent kinds of such interactions are observed. The first one (In2–In1–In2) is formed by In atoms only within the CeIn_3 segment (Fig. 4, left), two others (In1–Ir–In1) are found within the IrIn_2 segment (Fig. 4, middle and right). The last (sixth) shell of Ce is absent suggesting an electron transfer to the Ir–In framework (ionic interaction); the non-spherical Electron-Localizability-Indicator (ELI, Υ) distribution in the fifth shell indicates that these electrons also participate in the interaction within the valence region. Recent investigations of the atomic arrangements at the surface of single crystals of intermetallic compounds $\text{Al}_{13}\text{Co}_4$ (Ref. 38, 39) and $\text{Al}_{13}\text{Fe}_4$ (Ref. 40) reveal that the terminating surface often exhibits a large amount of covalent bonds.

Applying this approach to CeIrIn_5 we found that there are likely three different crystallographic planes along which the compound may preferentially cleave: the $\{100\}$ planes containing In2–In1–In2 bonds, and the $\{001\}$ and $\{113\}$ planes containing In1–Ir–In1 interactions. Most likely for reasons of the bond strength, in CeIrIn_5 the $\{113\}$ planes are expected to be the terminating ones upon cleaving, whereas in CeCoIn_5 —

showing very similar atomic interactions—the $\{001\}$ planes were found [23, 24, 35] as the terminating ones after cleaving. Because the $\{113\}$ planes are present in four different orientations in the crystal, the cleavage of CeIrIn_5 may not be regarded as similar to that in CeCoIn_5 .

Consequently, we suggest that the terminating surface seen in Fig. 2(a) is a $\{113\}$ plane. For such a plane an inclination of 37.2° with respect to the $\{001\}$ plane is expected, cf. Fig. 3(b), in good agreement with the inclination of the surface observed in STM. Within this plane the adjacent Ir atoms should be spaced by 6.6 \AA , Fig. 3(a). The distances of the **A**-type corrugations within the lines (e.g. line scan 1 in Fig. 2(a)) observed in STM topography, $(6.7 \pm 0.3) \text{ \AA}$, are in reasonable agreement with the shortest distances (i.e. along the $[110]$ direction) between the Ir atoms within the $\{113\}$ plane of CeIrIn_5 . Also, the nearest Ce atoms within this plane have the same distances which is consistent with the observation of analogous distances of corrugations **A** and **B** in Fig. 2(a). Within the $\{113\}$ plane and perpendicular to the $[110]$ direction, the next row of Ir (or Ce) atoms is located 12.43 \AA away, again in good agreement with our observation, cf. line scan 3 in Figs. 2(a) and (c). Here, however, there is an obvious difference between the HoCoGa₅ and TlAsPd₅ structure types: Within the HoCoGa₅ structure pattern the Ir atoms are shifted along $[110]$ such that the Ir atoms form isosceles triangles, as shown in Fig. 3(a), left. In contrast, the TlAsPd₅ structure pattern result in a rectangular arrangement of the Ir atoms, see Fig. 3(a), right. Clearly, both structure types are observed within the area of Fig. 2(a) as indicated by the dashed triangle and rectangle. Scan line 3 correspondingly follows a HoCoGa₅ structural pattern; the observed distance between corrugations of $(13.7 \pm 0.8) \text{ \AA}$ agrees nicely with the expected Ir distance of 12.86 \AA , see Fig. 3(a), left. Scan line 3 not only shows the prominent corrugations **A** but also the atoms of type **B** can be suspected.

Although the triangular arrangement of atoms **A** is much more dominant, we lack sufficient statistics in our STM topography to estimate the frequency of the two structure types and compare with to the result from XRD experiments. Moreover, the cleaving might have taken place along planes of increased defect density which may render a quantitative comparison between bulk-sensitive X-ray and surface-sensitive STM measurements difficult. The extent of the rectangular arrangement corresponding to the TlAsPd₅ structure pattern is, according to our STM topography, likely in the order of a few atomic distances. One might then speculate that the pattern of HoCoGa₅ structure type observed here are related to the structural imperfections which may cause the discrepancy between bulk and resistive superconducting transition temperature in CeIrIn_5 [21]. We note here that, although the total volume fraction of the impurity phase, i.e. the TlAsPd₅ structure pattern, is rather small, the physical properties might be influenced within a larger volume.

Recently, the intergrowth of α - and β -type YbAlB_4 single crystals was studied [41]. The latter compound is a heavy fermion superconductor exhibiting quantum criticality [42], with a specific heat coefficient being more than twice as large as in the α -type compound [43]. In β -type TmAlB_4 a sig-

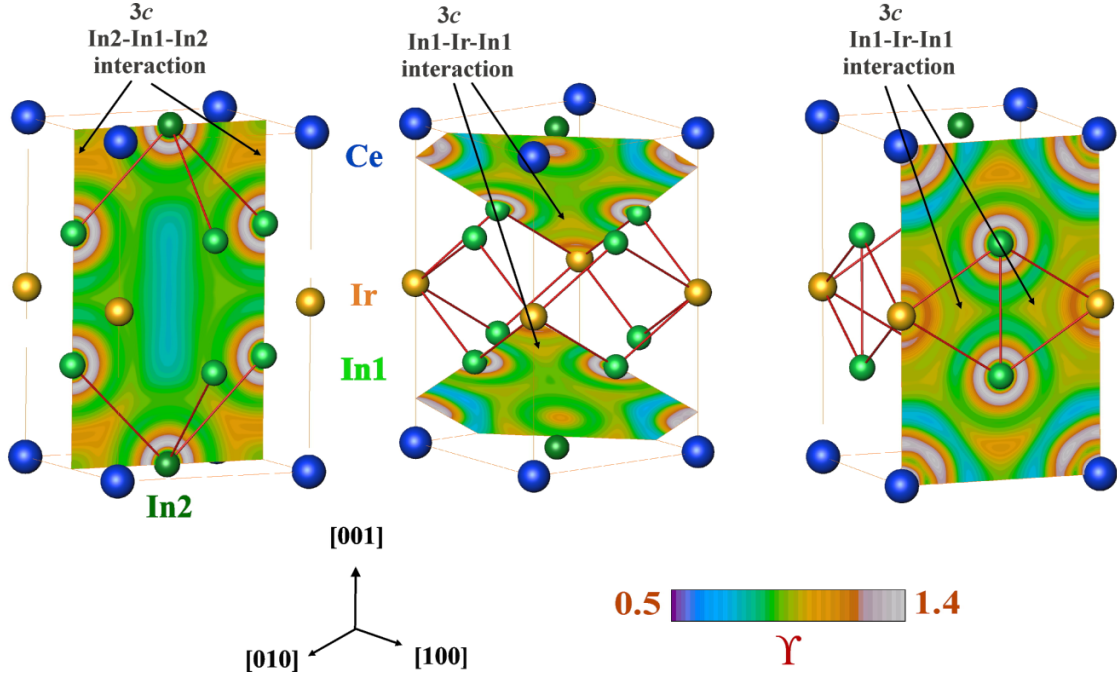


FIG. 4. Distribution of the Electron-Localizability-Indicator (ELI, γ) in CeIrIn_5 revealing the 3c interactions within the anionic Ir-In framework, and mostly ionic interactions of the Ce cations with the framework.

nificantly enhanced magnetic interaction was found [44] if compared to its α -type counterpart. These observations again underline the importance of detailed structural investigations for shedding light on intricate physical properties. We attempted to conduct Scanning Tunneling Spectroscopy (STS) within the atomically resolved surface areas of our CeIrIn_5 to possibly identify differences in the physical properties of the HoCoGa_5 and TlAsPd_5 structure types. However, no significant differences were found. Specifically, no indication for the opening of a superconducting gap was observed in the measured tunneling conductance within neither areas, independent of whether they belong to the HoCoGa_5 or the TlAsPd_5 structure types. Therefore, possible differences in the superconducting properties of the two different structure types could, unfortunately, not directly be visualized. We speculate that superconductivity may be diminished at the sample surface. We also note that our measurement base temperature $T = 0.32$ K is just below the bulk $T_c \approx 0.4$ K.

V. PRECURSOR STATE TO SUPERCONDUCTIVITY

For CeCoIn_5 with $T_c \approx 2.3$ K the situation is much more comfortable, and the formation of heavy fermions and of superconductivity was investigated by STS [23, 24, 35]. As mentioned above, however, all our attempts to cleave (more than 30) and those reported [23, 24, 35] resulted in surfaces with terraces of $\{001\}$ orientation rendering the observation of a possible similar TlAsPd_5 structure pattern in CeCoIn_5 highly difficult. Consequently, a direct visualization of the two different structure types as found for CeCoIn_5 by XRD

investigations was not possible.

Earlier magnetotransport investigations on the system CeIrIn_5 indicated the existence of a precursor state to superconductivity [22]. Moreover, it was demonstrated that the Hall coefficient R_H and the magnetoresistance ρ_{xx} are governed by two distinct scattering times [45]. Both observations are reminiscent of the behavior found for the copper oxide superconductors and are consistent with a scenario in which incipient antiferromagnetic fluctuations crucially influence the magnetotransport in both classes of materials, the fermion systems as well as the cuprates. In case of the cuprate superconductors, STS has proven to be a powerful tool for the investigation of the superconducting gap and, specifically, of the pseudogap [46]. Therefore, we investigated CeCoIn_5 by STS [34] with focus on a possible precursor state similar to the one found in CeIrIn_5 .

In Fig. 5(a), differential tunneling conductance ($g(V) = dI/dV$) spectra are presented as obtained for CeCoIn_5 within atomically flat terraces and within a temperature range $0.32 \text{ K} \leq T \leq 3 \text{ K}$. Upon increasing temperature the zero-bias conductance $g(V = 0)$ increases, indicating the expected closing of the gap. The gap, however, does not disappear at $T_c \approx 2.3$ K (bold red markers), but is still clearly visible at $T = 3$ K. We note that the observed gap is genuine in that the application of a small magnetic field of $\mu_0 H = 0.1$ T perpendicular to the sample surface does not alter the gap spectrum notably, see Fig. 5(b). The observation of coherence peaks at lowest temperatures may indicate that these gap structures are indeed related to superconductivity, rather than to Kondo interactions [35, 47]. This assessment is corroborated by the temperature dependence of the relative depth of the gap, Fig.

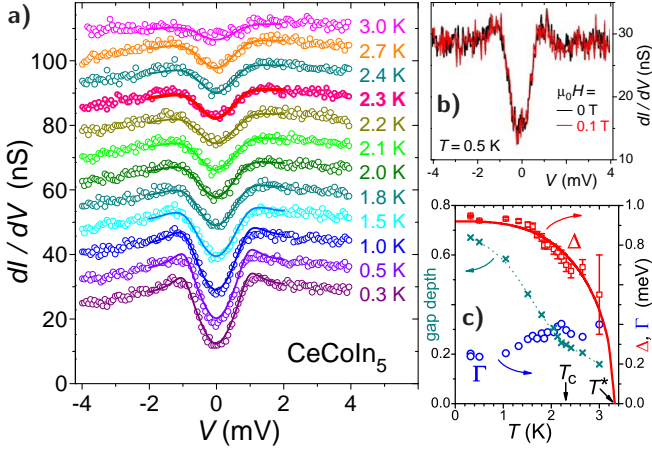


FIG. 5. Tunneling spectroscopy on CeCoIn₅. a) Measured tunneling conductance $g(V) = dI/dV$ (open circles, set point parameters: $V = +14$ mV, $I_{\text{set}} = 340$ pA), for clarity shifted vertically (except the one obtained at $T = 0.3$ K). The lines are results of the fit at each temperature (see text). b) Comparison of $g(V) = dI/dV$ for zero field and $\mu_0 H = 0.1$ T. c) Values of $\Delta(T)$ and $\Gamma(T)$ resulting from the fits of the tunneling conductance at each measured temperature in a). Also shown is the relative depth of the gap (see text).

5(c), which does not exhibit the logarithmic decay expected [48] for Kondo systems. Here, the gap depth was taken as the difference in conductance $g(V)$ at the coherence peaks (*i.e.* around $|V| \approx 1.1$ mV) and at $V = 0$, normalized to $g(V = -4$ mV) (*i.e.* away from the gap structure) after subtracting a linear background.

Assuming a $d_{x^2-y^2}$ symmetry of the superconducting order parameter as suggested elsewhere [23, 24, 49, 50], the tunneling density of state (which is directly related to $g(V) = dI/dV$) within the BCS framework is given by [51]

$$\rho(E) \propto \text{Re} \int_0^{2\pi} \frac{d\phi}{2\pi} \frac{E - i\Gamma}{\sqrt{(E - i\Gamma)^2 - \Delta^2 \cos^2(2\phi)}}. \quad (1)$$

Here, Δ is the maximum value of the angular dependent gap function and Γ is an additional lifetime broadening parameter. For each measured temperature the resulting fit is included as line in Fig. 5(a) while the values of Δ and Γ are presented in Fig. 5(c). As expected, Γ shows only little temperature dependence (its low-temperature value of 0.25 meV is in accord with results from point contact spectroscopy [52]) while Δ decreases with temperature. For nodal superconductors, the temperature dependence of the order parameter can be approximated [53] by $\Delta(T) = \Delta_0 \sqrt{1 - (T/T^*)^3}$. The red line in Fig. 5(c) represents a corresponding fit of our results which yields $T^* \approx 3.3$ K as the temperature at which the order parameter vanishes.

The zero-temperature value of the order parameter $\Delta_0 \approx 0.93$ meV results in $2\Delta_0/k_B T_c \approx 9.3$. Although such large values have been reported [54, 55], smaller numbers [56] of ~ 6 appear more reliable. A range of Δ_0 values was suggested to result from the quality of the sample surface [57]. Indeed, recent STM investigations [24] showed the development of a pseudogap-like feature just above 5 K, but only on one type

of surface (for the superconducting gap at lower temperature, $\Delta_{\text{SC}} \approx 0.6$ meV was reported [23, 24]). Note that our data do not provide any indication for multiple order parameters [55].

In the following we focus on the appearance of a pseudogap-like feature above T_c which is estimated to dissolve around 3.3 K. A pseudogap refers to a metallic regime within the temperature range $T_c < T < T^*$ where the DOS is considerably suppressed at least in parts of the Brillouin zone [58]. At least for the cuprate superconductors, the d -wave nature of the order parameter holds for the superconducting and the pseudogap regime [58, 59] suggesting that the above defined T^* (vanishing order parameter) equivalently limits the pseudogap regime towards higher temperatures. Pseudogaps have been observed in a number of systems displaying electronically mediated superconductivity. The pseudogap regime was first discovered in hole-doped cuprates where NMR measurements pointed to pseudo-gapped spin excitations [60]. It subsequently was seen by photoemission and detected in transport measurements (see *e.g.* Ref. 58 for details on the pseudogap regime in the cuprates). Similar pseudogap regimes have also been seen in other unconventional superconductors belonging to the iron pnictide family [61] and the organic transfer salt superconductors [62].

As the pseudogap feature evolves smoothly out of the superconducting regime it is tempting to suspect an analogy to the precursor state to superconductivity found [22] in CeIrIn₅ as well as the pseudogap reported [63] for CeRhIn₅ in a pressure regime where antiferromagnetism and superconductivity coexist. A pseudogap-like feature was speculated to exist in CeCoIn₅ up to 3.3 K at ambient pressure based on measurements of electrical resistivity under pressure [64]. Also, the fourfold anisotropy expected for a d -wave superconductor was observed up to 3.2 K [49].

An interpretation of the pseudogap formation as a precursor phenomenon to unconventional superconductivity may appear natural as the suppression of the DOS at temperatures $T_c < T < T^*$ reduces the kinetic energy increase that accompanies the opening of a full charge excitation gap at T_c . Indeed, a suppression of the normal-state DOS is a consequence of incoherent pairing above T_c , a phenomenon which is more pronounced in superconductors with short coherence lengths. T^* then marks the crossover energy scale to a regular metallic DOS. Yet, the origin and nature of the T^* -line, and concomitantly the pseudogap regime in (primarily) the cuprates has remained controversial [65]. According to some theories, T^* is associated with a sharp phase transition into an ordered state out of which superconductivity arises. Competing interactions, *e.g.* superconductivity and charge density wave order seem quite generally to promote the suppression of the DOS above T_c . A recent numerical study of the single-band Hubbard model based on the cluster dynamical mean field theory with clusters containing up to 16 sites finds that the pseudogap regime itself competes with superconductivity and that the superconductivity in this model tends to reduce the charge excitation gap when it emerges from the pseudogap phase [66]. The pseudogap phase in the Hubbard model separates a Mott insulator from the superconducting ground state.

The pseudogap regime in CeCoIn₅ thus seems to be of a dif-

ferent origin than the one in the cuprates as superconductivity in CeCoIn_5 does not arise near a Mott transition, but instead in close proximity of a spin-density wave quantum critical point. The coherence length ξ in CeCoIn_5 is only about 48 Å [24, 67], so that the pseudogap regime may rather be caused by incoherent pairing. The situation is different for CeRhIn_5 , where superconductivity is found near the onset of magnetism that is characterized by a critical Kondo destruction [68]. This local quantum criticality is associated with a Mott-like localization of the $4f$ -moments [69]. The observation [63] of a pseudogap regime accompanying superconductivity in CeRhIn_5 thus helps to elucidate the role kinetic energy gain at T_c plays in unconventional superconductors. For spin-fluctuation mediated superconductors this question has recently been raised in the context of CeCu_2Si_2 [70, 71]. A better understanding of the occurrence and origin of the pseudogap regime in heavy fermion superconductors may thus foster a deeper understanding of the intricate interplay between superconductivity and magnetism that apparently underlies almost all electronically driven superconductors.

VI. CONCLUSION

The investigated single crystals of CeIrIn_5 exhibited a co-existence of the expected HoCoGa_5 -type majority structural pattern with a minority pattern (1.2%) of the TlAsPd_5 type. Here, the combination of different techniques proved essential: While the XRD measurements showed that these structural impurities are present throughout the bulk of the samples (not just at their surfaces) the STM investigations directly visualized these latter, additional structural patterns at the surface. Clearly, such “structural impurities” are to be expected whenever very closely related structure types can be realized within a given compound, and should be borne in mind in the consideration of complex physical properties.

ACKNOWLEDGEMENTS

This work is partially supported by the German Research Foundation through DFG Forschergruppe 960. Z.F. acknowledges support through NSF-DMR-0801253. Work at Los Alamos was performed under the auspices of the US DOE, Office of Basic Energy Sciences, Division of Materials Sciences and Engineering.

-
- [1] J. Kondo: Prog. Theo. Phys. **32** (1964) 37.
 - [2] L. D. Landau: Sov. Phys. JETP **3** (1957) 920.
 - [3] S. Doniach: Physica B **91** (1977) 231.
 - [4] Q. Si and F. Steglich: Science **329** (2010) 1161.
 - [5] N. D. Mathur, F. M. Grosche, S. R. Julian, I. R. Walker, D. M. Freye, R. K. W. Haselwimmer and G. G. Lonzarich: Nature **394** (1998) 39.
 - [6] D. M. Broun: Nature Phys. **4** (2008) 170.
 - [7] J. Bardeen, L. N. Cooper and J. R. Schrieffer: Phys. Rev. **108** (1957) 1175.
 - [8] J. L. Sarrao and J. D. Thompson: J. Phys. Soc. Jpn. **76** (2007) 051013.
 - [9] J. D. Thompson and Z. Fisk: J. Phys. Soc. Jpn. **81** (2012) 011002.
 - [10] T. Park, V. A. Sidorov, F. Ronning, J.-X. Zhu, Y. Tokiwa, H. Lee, E. D. Bauer, R. Movshovich, J. L. Sarrao and J. D. Thompson: Nature **456** (2008) 366.
 - [11] C. Stock, C. Broholm, J. Hudis, H. J. Kang and C. Petrovic: Phys. Rev. Lett. **100** (2008) 087001.
 - [12] J. Paglione, M. A. Tanatar, D. G. Hawthorn, E. Boaknin, R. W. Hill, F. Ronning, M. Sutherland, L. Taillefer, C. Petrovic and P. C. Canfield: Phys. Rev. Lett. **91** (2003) 246405.
 - [13] A. Bianchi, R. Movshovich, I. Vekhter, P. G. Pagliuso and J. L. Sarrao: Phys. Rev. Lett. **91** (2003) 257001.
 - [14] S. Singh, C. Capan, M. Nicklas, M. Rams, A. Gladun, H. Lee, J. F. DiTusa, Z. Fisk, F. Steglich and S. Wirth: Phys. Rev. Lett. **98** (2007) 057001.
 - [15] S. Zaum, K. Grube, R. Schäfer, E. D. Bauer, J. D. Thompson and H. von Löhneysen: Phys. Rev. Lett. **106** (2011) 087003.
 - [16] T. Hu, H. Xiao, T. A. Sayles, M. Dzero, M. B. Maple and C. C. Almasan: Phys. Rev. Lett. **108** (2012) 056401.
 - [17] Y. Tokiwa, E. D. Bauer and P. Gegenwart: Phys. Rev. Lett. **111** (2013) 107003.
 - [18] R. R. Urbano, B.-L. Young, N. J. Curro, J. D. Thompson, L. D. Pham and Z. Fisk: Phys. Rev. Lett. **99** (2007) 146402.
 - [19] S. Nair, O. Stockert, U. Witte, M. Nicklas, R. Schedler, K. Kiefer, J. D. Thompson, A. D. Bianchi, Z. Fisk, S. Wirth and F. Steglich: Proc. Natl. Acad. Sci. USA **107** (2010) 9537.
 - [20] C. Petrovic, R. Movshovich, M. Jaime, P. G. Pagliuso, M. F. Hundley, J. L. Sarrao, Z. Fisk and J. D. Thompson: Europhys. Lett. **53** (2001) 354.
 - [21] A. D. Bianchi, R. Movshovich, M. Jaime, J. D. Thompson, P. G. Pagliuso and J. L. Sarrao: Phys. Rev. B **64** (2001) 220504(R).
 - [22] S. Nair, S. Wirth, M. Nicklas, J. L. Sarrao, J. D. Thompson, Z. Fisk and F. Steglich: Phys. Rev. Lett. **100** (2008) 137003.
 - [23] M. P. Allan, F. Massee, D. K. Morr, J. van Dyke, A.W. Rost, A. P. Mackenzie, C. Petrovic and J. C. Davis: Nature Phys. **9** (2013) 468.
 - [24] B. B. Zhou, S. Misra, E. H. da Silva Neto, P. Aynajian, R. E. Baumbach, J. D. Thompson, E. D. Bauer and A. Yazdani: Nature Phys. **9** (2013) 474.
 - [25] E. G. Moshopoulou, Z. Fisk, J. L. Sarrao and J. D. Thompson: Solid State Chem. **158** (2001) 25.
 - [26] Yu. Grin, Ya. P. Yarmolyuk and E. I. Gladyshevski: Sov. Phys. Crystallogr. **24** (1979) 137.
 - [27] T. Mori, H. Borrmann, S. Okada, K. Kudou, A. Leithe-Jasper, U. Burkhardt and Yu. Grin: Phys. Rev. B **76** (2007) 064404.
 - [28] K. Yubuta, T. Mori, A. Leithe-Jasper, Yu. Grin, S. Okada and T. Shishido: Mater. Res. Bull. **44** (2009) 1743.
 - [29] M. El-Boragy and K. Schubert: Z. Metallkd. **61** (1970) 579.
 - [30] M. Wedel and H. Borrmann: Acta Crystallogr. **A68** (2012) s81.
 - [31] Structural data for CeIrIn_5 : space group $P4/mmm$; $a = 4.6660(3)$ Å, $c = 7.5161(7)$ Å; 1Ce in $1(a) 0 0 0$, $B_{eq} = 0.65(1)$; 4In1 in $4(i) 0 \frac{1}{2} 0.30535(7)$, $B_{eq} = 0.95(1)$; 1In2 in $1(c) \frac{1}{2} 0 0$, $B_{eq} = 0.9(2)$; 0.986(2)Ir1 in $1(b) 0 0 \frac{1}{2}$, $B_{eq} = 0.74(1)$; 0.014(2)Ir2 in $1(d) \frac{1}{2} \frac{1}{2} \frac{1}{2}$, $B_{iso} = 0.8(1)$; $R(F) = 0.016$ for

- 240 observed symmetrically independent reflections; $B_{eq} = 1/3[B_{11}a^{*2}a^2 + \dots 2B_{23}b^*c^*bc \cos \alpha]$; B_{iso} stands for the isotropic displacement parameter of Ir2, all other atoms were refined in anisotropic approximation of the atomic displacement.
- [32] Y. M. Kalychak, V. I. Zaremba, V. M. Baranyak, V. A. Bruskov and P. Y. Zavali: *Russ. Metall.* **1** (1989) 213.
- [33] Structural data for CeCoIn₅: space group $P4/mmm$; $a = 4.6132(5)$ Å, $c = 7.748(1)$ Å; 1Ce in $1(a) 0 0 0$, $B_{eq} = 0.73(2)$; 4In1 in $4(i) 0 \frac{1}{2} 0.3095(1)$, $B_{eq} = 1.04(2)$; 1In2 in $1(c) \frac{1}{2} \frac{1}{2} 0$, $B_{eq} = 0.94(3)$; 0.985(8)Co1 in $1(b) 0 0 \frac{1}{2}$, $B_{eq} = 0.74(1)$; 0.015(8)Co2 in $1(d) \frac{1}{2} \frac{1}{2} \frac{1}{2}$, $B_{iso} = 0.8(1)$; $R(F) = 0.032$ for 1001 observed reflections, refinement including the symmetrically independent reflections only was instable; $B_{eq} = 1/3[B_{11}a^{*2}a^2 + \dots 2B_{23}b^*c^*bc \cos \alpha]$; B_{iso} stands in this case for the isotropic displacement parameter of Co2, all other atoms were refined in anisotropic approximation of the atomic displacement.
- [34] S. Ernst, S. Wirth, F. Steglich, Z. Fisk, J. L. Sarrao and J. D. Thompson: *Phys. Status Solidi B* **240** (2010) 624.
- [35] P. Aynajian, E. H. da Silva Neto, A. Gyenis, R. E. Baumbach, J. D. Thompson, Z. Fisk, E. D. Bauer and A. Yazdani: *Nature* **486** (2012) 201.
- [36] R. F. W. Bader: *Atoms in Molecules, A Quantum Theory* (Clarendon Press and Oxford University Press, New York, 1994).
- [37] F. R. Wagner, M. Kohout and Yu. Grin: *J. Phys. Chem. A* **112** (2008) 9814.
- [38] R. Addou, E. Gaudry, T. Deniozou, M. Heggen, M. Feuerbacher, P. Gille, Yu. Grin, R. Widmer, O. Gröning, V. Fournée, J.-M. Dubois and J. Ledieu: *Phys. Rev. B* **80** (2009) 014203.
- [39] H. Shin, K. Pussi, E. Gaudry, J. Ledieu, V. Fournée, S. Alarcón Villaseca, J.-M. Dubois, Yu. Grin, P. Gille, W. Moritz and R. D. Diehl: *Phys. Rev. B* **84** (2011) 085411.
- [40] J. Ledieu, E. Gaudry, L. N. Serkovic Loli, S. Alarcón Villaseca, M.-C. de Weerd, M. Hahne, P. Gille, Yu. Grin, J.-M. Dubois and V. Fournée: *Phys. Rev. Lett.* **110** (2013) 076102.
- [41] K. Yubuta, T. Mori, S. Okada, Yu. Prots, H. Borrmann, Yu. Grin and T. Shishido: *Phil. Mag.* **93** (2013) 1054.
- [42] S. Nakatsuji, K. Kuga, Y. Machida, T. Tayama, T. Sakakibara, Y. Karaki, H. Ishimoto, S. Yonezawa, Y. Maeno, E. Pearson, G. G. Lonzarich, L. Balicas, H. Lee and Z. Fisk: *Nature Phys.* **4** (2008) 603.
- [43] R. T. Macaluso, S. Nakatsuji, K. Kuga, E. L. Thomas, Y. Machida, Y. Maeno, Z. Fisk and J. Y. Chan: *Chem. Mater.* **19** (2007) 1918.
- [44] T. Mori, T. Shishido, K. Yubuta, K. Nakajima, A. Leithe-Jasper and Yu. Grin: *J. Appl. Phys.* **107** (2010) 09E112.
- [45] S. Nair, M. Nicklas, J. L. Sarrao, J. D. Thompson, F. Steglich and S. Wirth: *J. Supercond. Nov. Magn.* **22** (2009) 201.
- [46] Ø. Fischer, M. Kugler, I. Maggio-Aprile, C. Berthod and C. Renner: *Rev. Mod. Phys.* **79** (2007) 353.
- [47] S. Ernst, S. Kirchner, C. Krellner, C. Geibel, G. Zwicknagl, F. Steglich and S. Wirth: *Nature* **474** (2011) 362.
- [48] T. A. Costi: *Phys. Rev. Lett.* **85** (2000) 1504.
- [49] K. Izawa, H. Yamaguchi, Y. Matsuda, H. Shishido, R. Settai and Y. Ōnuki: *Phys. Rev. Lett.* **87** (2001) 057002.
- [50] A. Vorontsov and I. Vekhter: *Phys. Rev. Lett.* **96** (2006) 237001.
- [51] H. Won and K. Maki: *Phys. Rev. B* **49** (1994) 1397.
- [52] W. K. Park, L. H. Greene, J. L. Sarrao and J. D. Thompson: *Phys. Rev. B* **72** (2005) 052509.
- [53] B. Dóra and A. Virostek: *Eur. Phys. J. B* **22** (2001) 167.
- [54] G. Goll, H. v. Löhneysen, V. S. Zapf, E. D. Bauer and M. B. Maple: *Acta Phys. Pol. B* **34** (2003) 575.
- [55] P. M. C. Rourke, M. A. Tanatar, C. S. Turel, J. Berdeklis, C. Petrovic and J. Y. T. Wei: *Phys. Rev. Lett.* **94** (2005) 107005.
- [56] W. K. Park, J. L. Sarrao, J. D. Thompson and L. H. Greene: *Phys. Rev. B* **72** (2005) 052509.
- [57] A. Sumiyama, R. Onuki, Y. Oda, H. Shishido, R. Settai and Y. Ōnuki: *J. Phys. Chem. Solids* **69** (2005) 3018.
- [58] T. Timusk and B. Statt: *Rep. Prog. Phys.* **62** (1999) 61.
- [59] T. Valla, A. V. Fedorov, J. Lee, J. C. Davis and G. D. Gu: *Science* **314** (2006) 1914.
- [60] W. W. Warren Jr., R. E. Walstedt, J. F. Brennert, R. J. Cava, R. Tycko, R. F. Bell and G. Dabbagh: *Phys. Rev. Lett.* **62** (1989) 1193.
- [61] Y.-M. Xu, P. Richard, K. Nakayama, T. Kawahara, Y. Sekiba, T. Qian, M. Neupane, S. Souma, T. Sato, T. Takahashi, H.-Q. Luo, H.-H. Wen, G.-F. Chen, N.-L. Wang, Z. Wang, Z. Fang, X. Dai and H. Ding: *Nature Comm.* **2** (2011) 392.
- [62] J. Kang, S.-L. Yu, T. Xiang and J.-X. Li: *Phys. Rev. B* **84** (2011) 064520.
- [63] S. Kawasaki, M. Yashima, T. Mito, Y. Kawasaki, G.-q. Zheng, Y. Kitaoka, D. Aoki, Y. Haga and Y. Ōnuki: *J. Phys.: Condens. Matter* **17** (2005) S889.
- [64] V. A. Sidorov, M. Nicklas, P. G. Pagliuso, J. L. Sarrao, Y. Bang, A. V. Balatsky and J. D. Thompson: *Phys. Rev. Lett.* **89** (2002) 157004.
- [65] A. J. Millis: *Science* **314** (2006) 1888.
- [66] E. Gull, O. Parcollet and A. J. Millis: *Phys. Rev. Lett.* **110** (2013) 216405.
- [67] T. Tayama, A. Harita, T. Sakakibara, Y. Haga, H. Shishido, R. Settai, and Y. Ōnuki: *Phys. Rev. B* **65** (2002) 180504(R).
- [68] Tuson Park, F. Ronning, H. Q. Yuan, M. B. Salamon, R. Movshovich, J. L. Sarrao and J. D. Thompson: *Nature* **440** (2006) 65.
- [69] Q. Si, S. Rabello, K. Ingersent and J. L. Smith: *Nature* **413** (2001) 804.
- [70] O. Stockert, J. Arndt, E. Faulhaber, C. Geibel, H. S. Jeevan, S. Kirchner, M. Loewenhaupt, K. Schmalzl, W. Schmidt, Q. Si and F. Steglich: *Nature Phys.* **7** (2011) 119.
- [71] O. Stockert, S. Kirchner, F. Steglich and Q. Si: *J. Phys. Soc. Jpn.* **81** (2012) 011001.